Carpathian Journal of Earth and Environmental Sciences, February 2021, Vol. 16, No. 1, p. 151 – 162; Doi:10.26471/cjees/2021/016/163

STRUCTURAL CHARACTERIZATION OF A BENTONITE DEPOSIT FROM THE EASTERN IRAN; COMPARISON WITH TWO REFERENCE BENTONITES

Samira DOLATI[1*] & Mohsen KALANI[2]

[1]Department of Chemistry, Dezful Branch, Islamic Azad University, Dezful, Iran
**Corresponding author: e-mail: samira.dolati@gmail.com*
[2]Department of Geology, National Iranian South Oil Company, Ahvaz, Iran

Abstract: Mineralogically, bentonites are dominated by smectites and due to characteristic textural and physicochemical properties of smectites (e.g. very small particle sizes, high cation exchange capacity) are of a great use in industrial applications. In this study, a bentonite sample was characterized with regard to the particle size distribution, mineralogical composition and cation exchange capacity in comparison with the data for the two internationally well-known bentonites representative for Na- and Ca-bentonites: the Mx-80 bentonite of Wyoming, USA and that of Milos, Greece, respectively. Results show a high fraction of fine-grained particles, which demonstrates high yield of purified clay. Mineralogically, the studied bentonite comprises mainly smectites and expandable illite-smectite mixed layer clay minerals. Main accessory minerals are calcite, silica polymorphs and zeolites. The specific surface area and cation exchange capacity values are 330.3(m^2 g^{-1}) and 42.2 (meq/ 100 g), respectively. It is concluded that the mineralogical, textural and the measured physicochemical properties of the studied bentonite is applicable to the applications in oil industry and its related environment maintenance related issues.

Keywords: bentonite; grain size distribution; cation exchange capacity; X-ray powder diffraction; Fourier Transform Infra-Red spectroscopy.

1. INTRODUCTION

Bentonite is a lithological term used to describe clay materials originated from alteration of volcanic tuffs and ashes (Ross & Shannon, 1926). Nevertheless, more recently, the term is applied to any clay material, which is dominantly composed of smectites minerals regardless of its origin (Grim & Güven, 1978; Murray, 2006).

Bentonites are formed and stable at Earth's surface conditions. However, different climate and hydrological regime as well as different ages and depths of occurrence cause notable variations in compositional, mineralogical and consequently physicochemical properties of this material (Murray, 2006; Odom, 1984).

Smectites are hydrous aluminum silicates, which comprise 2:1 structures, composed of two silica tetrahedral sheets sandwiching an octahedral sheet (e.g. Odom, 1984). Notable cation substitutions of Fe^{+2}, Fe^{3+}, and Mg^{2+} for Al^{3+}, and less importantly some substitutions of silicon by aluminum in tetrahedral sheets, cause a net positive charge deficiency. The positive charge deficiency is balanced by exchangeable cations absorbed between the structural layers and the edges.

Based on the exchangeable cations, the smectites varieties form, among which sodium montmorillonite, calcium montmorillonite, and hectorite are of wide industrial applications (e.g. Murray, 2006; Odom, 1984). Sodium and calcium are hydrated and hence associated with molecular water layers in the interlayer positions of the montmorillonites. High cation exchange capacity (CEC), and small size of the flakey texture, resulted in high swelling, high sorptivity and very high viscosity at low concentration, water impermeability, and thixotropy (i.e. ability to make gels when suspended in water) of sodium montmorillonite provide a wide spectrum of applications with regard to the energy sources development and its related environmental maintenance issues. It is widely used

in large quantities in drilling muds, as foundry bonds, and as absorbents (i.e. for filtration, clarifying and decolorizing and oil pollution removal purposes) (Murray, 2006; Odom, 1984). Na-montmorillonites have been shown to be suitable for being treated by the organic compounds to make organoclays with much larger lattice spacing and consequently higher absorbing capacities (Grim & Güven, 1978; Murray, 2006; Odom, 1984). In small quantities, however, purified natural (or chemically treated) Na-montmorillonite has been used to stabilize polymers planned to be injected to oil wells for enhanced oil recovery (EOR) purposes (Cheraghian, 2015).

The Wyoming, USA and Milos, Greece bentonites are instances of natural bentonites of constant structural and textural characteristics over several years of production and with wide industrial application spectra. Several authors have addressed different physicochemical properties, mineralogical compositions and textural characteristics of these samples (Carlson, 2010; Kumpulainen & Kiviranta, 2010; Kumpulainen & Kiviranta, 2011). One of the commercial clay products from the Wyoming bentonite is labeled as MX-80. The MX-80 comprises a sodium bentonite which is mineralogically dominated by Na-montmorillonite (Madejová et al., 2002). Milos bentonites of Greece comprise of the most important European bentonites (Carlson, 2010). The Milos bentonite is a calcium bentonite, which is mineralogically dominated by Ca-montmorillonite. In this work, we adapted the characteristics of these bentonites as the benchmarks to this study (Carlson, 2010; Kiviranta et al., 2018; Kumpulainen & Kiviranta, 2010). The MX-80 of Wyoming, USA and the Milos of Greece bentonite are here referred as Wyoming and Milos bentonites, respectively.

In this study the white-colored bentonite sample with high apparent swelling capacity, which promises wide usages in the energy, industry and its related environmental issues (as mentioned above) was characterized with regard to the particle size distribution, mineralogical composition and cation exchange capacity in comparison with the data for the two mentioned internationally well-known bentonites.

2. MATERIALS AND METHODS

2.1. Raw bentonite sample and purification

The raw bentonite sample comprises a white colored clay-rich material. This is a good quality representative sample of the bentonites occurring in the eastern bentonite zone of Iran (Hejazi & Ghorbani, 1994; Modabberi et al., 2015). This zone is largely associated with the Eocene volcanic rocks in general and tuffs in particular, extended over a wide area of the eastern Iran. Bulk mineralogy of the bentonite samples from different locations within the zone has been already reported, although detailed clay mineralogy is less investigated (Modabberi et al., 2015; Namayandeh et al., 2015). Furthermore, investigations showed a wide variability of bulk mineralogical compositions within the zone (Modabberi et al., 2015; Namayandeh et al., 2015) which highlights importance of further investigations.

Purification carried out by collection of the <2 µm fraction suspended in distilled water using settling tube according to Stokes´ law considering an average grain density of 2.5 gr $cm3^{-}$ for the non-clay fraction. Collected clay suspension was dewatered using either centrifugation or by passing through a membrane filter with 0.45 µm pore-size held in a filtration apparatus by applying vacuum. The dewatered sample was gently dehydrated in the oven at temperatures below 60°C for over 36 hours.

2.2. Particle-size analysis

Granular particle-size distribution was determined by wet-sieve method (Fritch model). Grain-size analysis of particles smaller than 63 µm was performed by the laser particle size analyzer. The laser particle size analyzer Analysette 22 provided by Fritsch GmbH deployed in this study works based on laser diffraction spectrometry.

2.3. Specific Surface area and cation exchange capacity

The methylene blue (MB) spot test method was used for determining the specific surface area (SSA) (Kandhal & Parker, 1998). The spot test provides a readily available technique for the determination of the specific surface of clays, including swelling clay minerals in the laboratory (Santamarina et al., 2002). The spot test also yields similar SSA values as spectrophotometry of titrated samples with methylene blue, to determine the amount of absorbed MB dose (Yukselen & Kaya, 2008). Assuming that the MB dye is capable of attaching to the exchange sites on the mineral surface by replacing the exchangeable cations, it is possible to translate the MB absorbance to the cation exchange capacity (CEC) values using the equation as proposed by Çokca and Birand (Çokca & Birand, 1993).

2.4. X-ray powder diffraction (XRPD)

X-ray powder diffraction (XRPD) mineralogical analysis carried out on both bulk

sample and clay fractions. Oriented clay mounts prepared out of the clay fraction were prepared using the filtration apparatus. Due to the high swelling and thixotropic properties of the extracted clay, preparation of the oriented mount was done with difficulty. The preparation was repeated until thick enough and uniform coverage of the whole glass was obtained. XRPD was measured on the Mg-saturated air-dried oriented mount, which was subsequently treated with ethylene glycol and heated to 350°C and 550°C following a procedure slightly modified after Poppe et al. (2001). The XRD patterns were measured using a PANalytical X'Pert Pro Multi-Purpose XRD System with CuKα radiation, and PIXcel0D detector, which provides high signal to noise ratio and allows high data collection speeds. The datasets were collected from 2 to 70 °2θ for bulk samples, and 2-35 °2θ for the oriented clay mount.

To quantify mineral composition, a semi-quantification or quantitative representation (QR) approach as summarized by Peltonen et al. (2008), was used. The QR approach is based on calculating the integrated peak area of mineral phases, multiplied by published weight factors. Based on this method, 'smectite' includes both smectites and randomly ordered mixed-layer illite-smectite (R0: 10–50% illite). The quantity of illite in the I-S was estimated based on the location of the 002/003 peak of illite/smectite (Moore & Reynolds, 1997).

2.5. Fourier Transform Infra-Red spectroscopy

The infra-red spectra of the whole and purified samples were acquired using a Thermo Nicolet iS10 FTIR spectrometer. The FTIR spectra were collected in the wavenumber range of 4000 to 400 cm^{-1} with a spectral resolution of 0.4 cm^{-1}. To prepare FTIR spectrometry pellets, 1mg of sample and 200 mg of KBr were mixed and pressed. No heat was applied to the pellets.

2.6. Scanning electron microscopy

Scanning electron microscopy (SEM) was performed on the gold-coated stubs prepared out of the raw bentonite sample as a complementary analysis for the mineralogical characterization. The secondary electron and backscattered electron images were obtained using a Hitachi XL30 Scanning Electron Microscope equipped with an Energy Dispersive X-ray (EDAX) spectrometer to identify the minerals in the samples.

3. RESULTS AND DISCUSSION

3.1. Particle size distribution

Particle size distribution is described and discussed in two sub-chapters: i) granulometric analysis of the whole rock and ii) the grain size distribution of the bulk sample, excluding the coarse fraction (> 1 mm).

3.1.1. Granulometric analysis

Table 1 and Figure 1 show the granular size distribution of the studied sample (BEI) and Wyoming and Milos reference bentonites. Comparison with the reference bentonites, the frequency of the coarse fraction (> 1 mm) in the BEI bentonite is much lower than that of the Milos bentonite and larger than the Wyoming bentonites. This is likely because the Wyoming bentonites (MX-80 in this case) are homogenized by the original producers (Carlson, 2010). Granulometric analysis also shows a very high fraction of fine particles (< 63 µm) which is around twenty and ten times higher than the same particle size range in the Wyoming and Milos bentonites, respectively.

Table 1. Whole rock granulometric analysis of particle distribution in the BEI (this study) and two reference clays (Kiviranta & Kumpulainen, 2011).

Granule size	BSE	Wyoming	Milos
> 2 mm	2.3	0	20.9
1 -2 mm	9.5	0.3	45.1
500µ - 1 mm	4.8	33.6	22.9
250- 500 µm	6.6	34	6.6
125 -250 µm	7.2	19.2	3.1
63- 12 5 µm	9.6	9.7	1.2
< 63 µm	60.0	3.2	0.3

The high yield of fine fraction in the BEI sample shows a notably finer texture of the studied bentonite. However, comparing this with the data adapted for the reference bentonites; it should be considered that the higher frequency of fine particles (< 63 µm) in this study is at least partly contributed by the higher efficiency of wet sieving technique than that of the traditional dry sieving, which was applied to the reference bentonites.

3.1.2. Particle size distribution of the bulk sample (excluding coarse fraction)

The measured particle size range in the BEI bentonite was 0.1 µm to 1885 µm. However, the coarse fraction was largely removed off from the sample fed into the automated particle size analyser (cf. materials and method chapter) causing the

frequency of particles larger than 100 µm counted negligible. Same conditions exist for the adapted data from the Wyoming and Milos bentonites. Therefore, direct comparison of results is possible (Fig. 2).

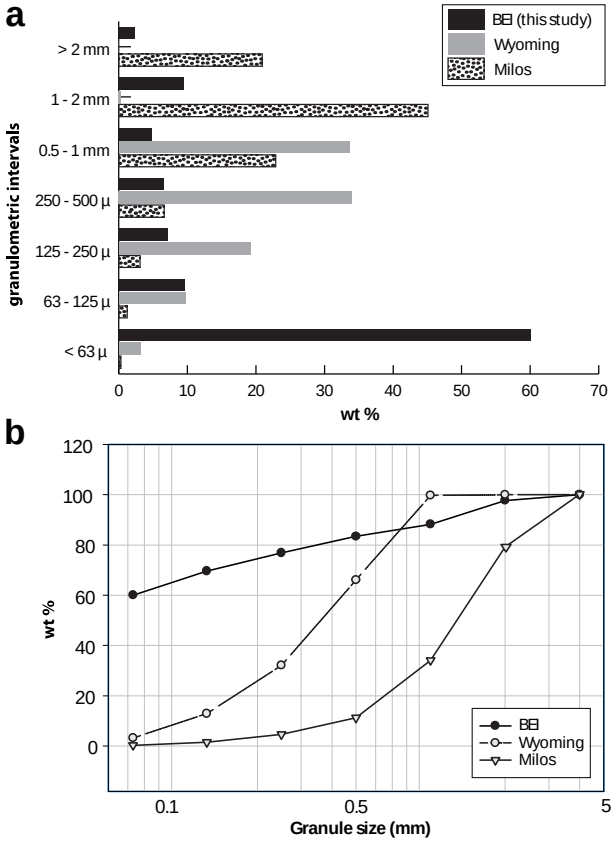

Figure 1. Whole rock granulometric analysis diagrams showing particle distribution in the BEI (this study) and two reference clays (Kiviranta & Kumpulainen, 2011). a) bar chart of fraction frequencies, b) cumulative frequency curves.

The particle size distribution forms a mono-modal frequency curve with a mode value of 6.7 µm. The frequency curve is asymmetric which means a non-normal distribution of particles. According to the cumulative frequency curve 80 wt% particles in the bulk BEI sample (excluding the coarse fraction) are ≤ 10 µm. The Wyoming sample shows similar distribution pattern for the same baulk fraction, although it forms a broader frequency curve, which means more uniform distribution of particle around the mode (6.7 µm). Nevertheless, as mentioned above frequency of particles below 100 µm is much lower in the Wyoming bentonite. The Milos bentonite, however, shows a bimodal frequency curve (4 and 20 µm) with much lower frequency of fine fractions (≤10 µm).

A direct comparison of cumulative frequencies of particle sizes in the bulk samples excluding the coarse fraction (> 1 mm) shows that with regard to fine fraction the BEI sample of this study is similar to the Wyoming bentonite and almost two times finer than the Milos bentonite. For example, 60 wt% of the particles in both BEI and Wyoming bulk samples fed into the automated particle size analyzer are ≤ 8 µm where the range comprises 30 % of the Milos bentonite. In addition, it is notable that ~ 97 wt% of the particles in the bulk sample are ≤ 20 µm. The same size range, however, comprises ~ 92 and 70 w% of the Wyoming and Milos reference bentonites, respectively.

3.2. Mineralogical analyses

3.2.1. X-ray powder diffraction (XRPD)

Figure 3a and b shows XRPD patterns of the bulk BEI sample (i.e. whole sample including the coarse fraction) and the clay fraction (< 2 µm), respectively. The bulk mineralogical results show that smectite is the prominent mineral. Furthermore Further, identification of clay minerals carried out based on the clay fraction-oriented mount as described below. In the BEI sample, calcite is the most important non-clay mineral. Silica polymorphs including quartz and opal C were identified by the XRPD. Opal C comprises relatively well-ordered stacking of α-cristobalite with minor evidences of tridymite stacking (Elzea et al., 1994; Graetsch et al., 1994). In the XRPD pattern, however, opal C resembles the α-cristobalite and diagnosis should carry out with consciousness and may involve further treatments. A quick check to distinguish opal C from α-cristobalite is to consider the width at half height (FWHD) of the (101) peak (i.e. peak close to 4.04 Å) of opaline silica polymorphs (Elzea et al., 1994). In the bulk sample of the BEI bentonite, d(101) peak is 4.052 Å. The FWHD of the peak is 0.49, which suggests that rather Opal C than the other opaline silica polymorphs exist (Fig. 3a).

Dominance of smectites is well documented by the XRPD of the oriented mound of the clay fraction (i.e. <2 µm) (Fig. 3b). The intense peak at 14.38 Å of the Mg-saturated air-dried sample which is expanded to 16.53 Å when treated by ethylene glycol largely represents smectites. When the oriented mount was subjected to heating, the peak collapsed partially treated at 350 °C and thoroughly at 550 °C. The peak, however, can also represent the expandable mixed layer I-S. Based on the position and/ or spacing of the illite 002 and smectite 003 reflection, it is suggested that the sample comprises randomly ordered intra-stratification of smectites and illites. Therefore, expandable mixed layer illite-smectite (I-S) is the second important clay mineral in BEI bentonite. Kaolinite and chlorites, however, do not exist.

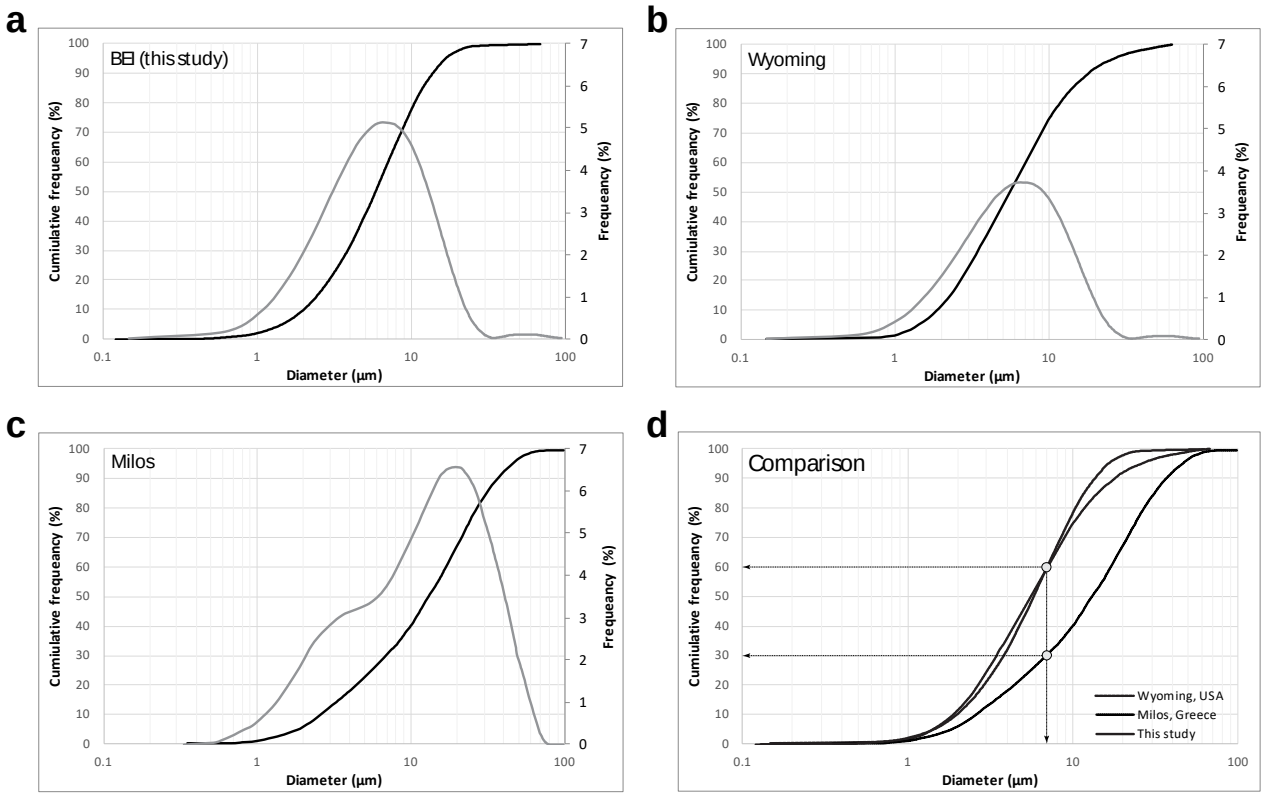

Figure 2. Particle size distribution of the bulk sample excluding the fraction > 1 mm. a) BEI (this study), b) Wyoming and, c) Milos (Kiviranta & Kumpulainen, 2011), d) comparison of cumulative frequencies of particle sizes.

Table 2. Lattice spacing, intensity, FWHM of representative peaks of respective minerals as well as QR results (i.e. relative frequencies, wt%).

Mineral	d-spacing(Å)	Intensity(cts)	FWHM (°2θ)	Frequency wt%
Quartz	3.35	1007.69	0.13	1.10
Calcite	3.04	5451.38	0.13	9.53
Opal C	4.05	3524.31	0.15	11.55
Zeolites (Tuffs)	9.33	156.84	0.05	1.37
Total clay**	4.49	2914.99	0.15	76.44

** comprises mainly smectite and expandable I-S (75.5 %) and trace amounts of illite (0.4 %) based on EG solvated oriented mount as below.

< 2 µm (EG)				
Smectite + R0 I-S	16.45	74357.52	0.28	98.83
Illite	10.41	301.43	0.20	0.53

Smectites type based on the d(060) of 1.50 Å is montmorillonite although minor contribution of nontronite is also possible (reflection at 60.6 °2θ; d(060) of 1.52) (Moore & Reynolds, 1997). Based on the d(001) reflection of 12.7 Å of the randomly oriented sample the montmorillonite is likely to be a Na type. Increasing of the basal spacing as represented by d(001) of the EG solvated oriented mount is inferred as the consequence of saturation with the divalent cation (Mg^{2+}) and may not be adapted for diagnosis of montmorillonite type.

Table 2 and 3 show quantitative representation (QR) of the mineral phases in the BEI bentonite sample and the mineralogical composition of the BEI when compared to adapted data of the reference bentonites, The different quantification approaches (i.e. calculating the integrated peak area of respective mineral phases in this study versus the Rietveld refinement for the adapted data of the reference bentonites), however, cause major uncertainties and

difficulties with regard to comparison of mineralogical compositions (Table 3). Nevertheless, the results show relatively lower smectite contents in the BEI bentonite.

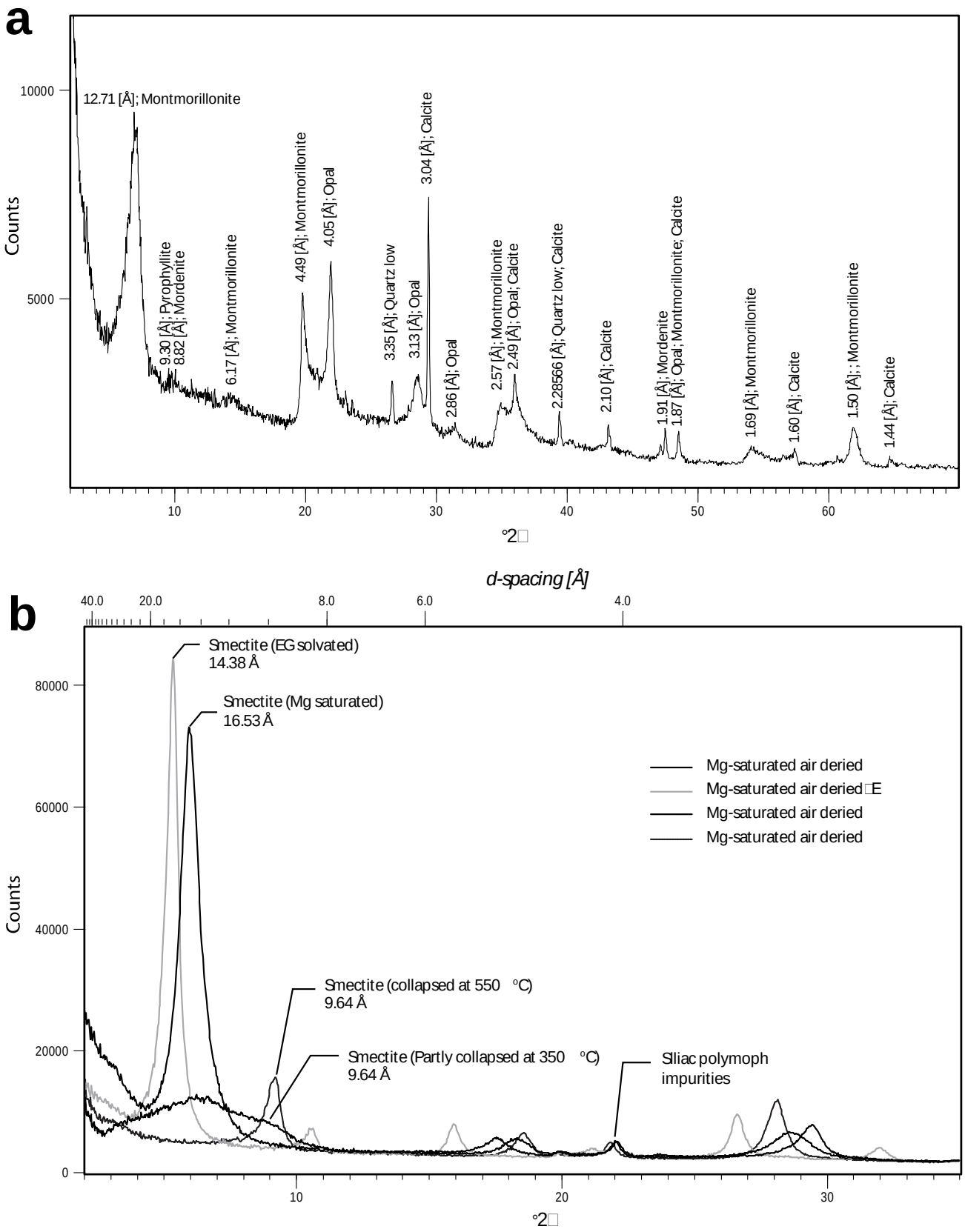

Figure 3. XRPD pattern and peak assignments. a) randomly oriented bulk sample, b) oriented mount of the clay fraction (< 2 μm).

Table 3. Comparison of estimated relative mineral frequencies of the BEI bentonite (this study) compared to mineralogical composition of the reference clays (Kiviranta & Kumpulainen, 2011). Wy= Wyoming, SM= smectite, IL= illite, QZ= quartz, Cris/OpC= cristobalite/opal C, Plg= plagioclases, Calc=calcite, Dol= dolomite, K-Feld=k-feldspars, Mic= mica, Chl= chlorite, Hem= hematite, Py=pyrite, OpA= Opal A, Rut=rutile, tr=trace amount.

	Sm	IL	QZ	Cris/ OpC	Plg	Calc	Dol	K-feld	Mic	Chl	Hem	Py	OpA	Rut
Wy	90.6	0.1	3.5	0.1	2.5	0.4		1.4	0.3	tr	tr	0.6		0.3
Milos	80.3	2.8	0.3		0.8	3.8	6.4	0.9	tr	1.4	0.7	1.4	0.5	0.5
BEI	75.5	0.4	1.10	11.55	tr	9.53			tr					

It should also be noted that in practice smectite quantified by the applied semi-quantification approach as well as the Rietveld refinement approach as presented by Kumpulainen & Kiviranta (2010), comprises both smectites and randomly interstratified illite-smectite: R0 illite (< 0.5)/smectite. With regard to the illite content in the randomly interstratified illite-smectite, the I-S d(002/003) of 5.56 Å suggests occurrence of R0 illite(0.24)/smectite in the sample. In other words, the I-S mineral (which was not quantified individually and was quantified in this study as a summation with smectite) has around 24 % illite in its structure.

3.2.2. Fourier Transform Infra-Red (FTIR) spectroscopy

Figure 4 shows FTIR spectra of the whole sample including both the coarse and fine fractions and the purified fraction (< 2 µm). Comparison of the spectra shows spectroscopic evidences of relatively effective elimination of non-clay minerals (as discussed below) and pre-dominance of clay minerals in the purified sample.

FTIR spectroscopy has been widely used to identify clay minerals for decades (Farmer & Russell, 1964; Heikola et al., 2013; Madejová, 2003; Madejová et al., 2002; Madejová & Komadel, 2001; Russell & Fraser, 1994). Accordingly, IR bands were assigned in this study. Table 4 shows the FTIR band assignments in the BEI whole and purified samples as compared with reference clays. On the FTIR spectra of the bulk and the purified clay of the BEI bentonite, band assignments are as follow: The IR band at 3622 cm^{-1} is assigned to stretching vibrations of structural hydroxyl groups (i.e. O-H stretching).

The bands corresponding to stretching vibration of Si-O groups are detected at around 1115 cm^{-1}. The IR absorption bands due to the Al-O-Si and Si-O–Si were observed at 529 and 465 cm^{-1} of the bulk sample's FTIR spectrum, respectively. The bending vibration of the cation associated hydroxyl groups of Al-Al-OH, Al-Fe-OH, Al-Mg-OH were observed at 911, 877, and 846 cm^{-1} of the FTIR spectrum of the bulk sample. The assigned bands as mentioned above are typical of montmorillonite. FTIR bands assignments are in high accordance with the XRPD mineralogical analysis.

Smectites (montmorillonite in our case) are highly water absorbents. Water absorbed by montmorillonite, caused IR bands at 3443 cm^{-1} (of the pure clay spectrum), corresponding to H_2O stretching vibrations. This is associated with a shoulder band at 3224 cm^{-1} (Table 4, Figure 4) assigned to the consequence of an overtone of the bending vibrations of the H_2O at 1460 cm^{-1} (Bishop et al., 1994; Madejová, 2003).

The most important IR bands associated with the non-clay minerals are as follow: the IR band at 1400 cm^{-1} in the bulk BEI sample FTIR spectrum is assigned to calcite. This is well supported by disappearance of the band in the FTIR spectrum of the purified sample. This is in agreement with the occurrence of calcite reflection in the XRPD pattern of the whole sample and their removal in the XRPD of the clay fraction-oriented mount. IR bands off silica polymorphs were observed at around 795 cm^{-1}. The latter, has been assigned to the platy form of tridymite by Russell & Fraser (1994).

We argue that this corresponds to tridymite stacking in association with α-cristobalite stacking of opal C in the FTIR spectrum of BEI sample. Nevertheless, Madejová & Komadel (2001) assigned the sharp IR absorbance band at 798 cm^{-1} of the Wyoming MX-80 bentonite to quartz. In addition, the IR absorbance band at around 625 cm^{-1} has been documented to be diagnostic of opal C (Curtis et al., 2019; Graetsch et al., 1994). The bulk sample FTIR spectrum also shows bands around 522-530cm^{-1} which are according to Curtis et al., (2019) are representative of highly amorphous silica polymorphs, although firmed x-ray diffraction evidence of Opal A was not observed. Therefore, the bands were assigned to free Si-O.

3.2.3. Scanning electron microscopy

SEM provides petrographic evidences of flaky

Table 4. FTIR band assignments for the BEI bentonite (this study) and two reference bentonites (Heikola et al., 2013; Kiviranta & Kumpulainen, 2011; Kumpulainen & Kiviranta, 2010).

		OH-stretching	**H2O-streching**	**overtone of H20 bending- vibration**	**H2O-bending**	**CO32– -stretching (Calcite)**	**Si–O stretching, Si-O-Si stretching,**	**Si–O stretching, tetrahedral Si (S, Q)**	**OH-bending, AlAlOH (S)**	**OH-bending, AlFeOH (S), (Calcite)**	**OH-bending, AlMgOH**	**Si–O stretching (Quartz, Cristobalite, free Si–O)**	**780: Si–O-bending (Quartz)**	**Si–O-bending (Quartz)**	**Si–O bending (Cristobalite)**	**Al–Si–O bending**	**Si–O–Si bending**
BEI	**Bulk**	3628	3443	3231	1636	1400	1114	1036	915	877	846	795	775	687	622	525	465
	Pure clay	3628	3445	3223	1640	–	1116	1038	911	881	846	796	785	–	621	522	464
Wyoming	**Bulk**	3636	~3433	–	~1624	~1382	1120	1043	919	884	846	796	–	694	623	526	466
	Pure clay	3637	3437	–	1623	1384	1119	1048	919	885	849	799	–	695	620	527	468
Milos	**Bulk**	3628	~3430	–	~1630	~1385	~1118	~1034	916	878	846	798	780	696	625	~525	~468
	Pure clay	3628	3438	–	1625	1384	1108	1035	919	882	845	801	–	700	618	525	468

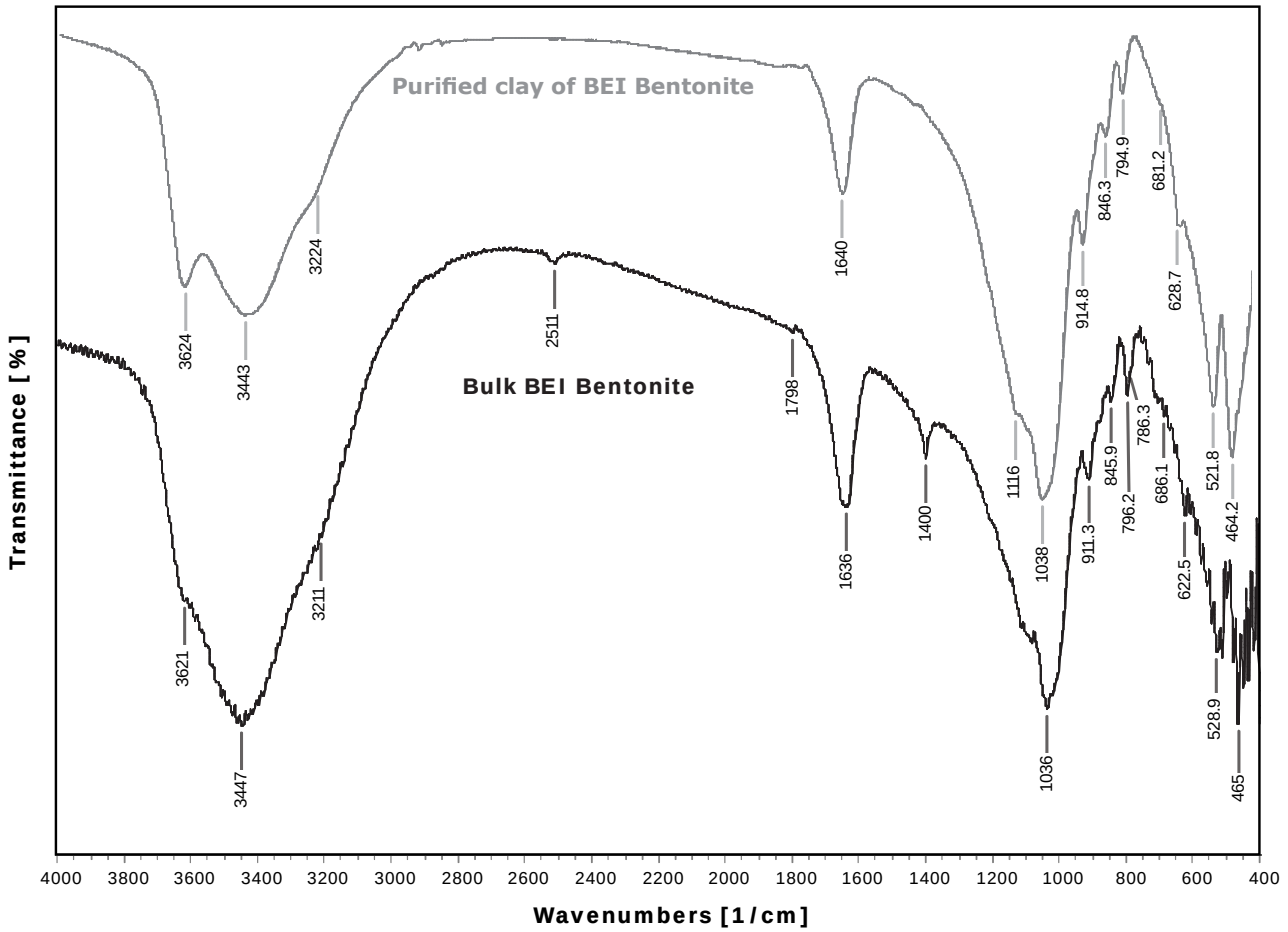

Figure 4. FTIR spectra of the Bulk BEI and purified clay of the same bentonite (this study) and major band assignments.

fabric of clay minerals (Fig. 5a) with EDS spectrum showing elements that can suggest montmorillonite (Na, Mg saturated) which is in accordance with XRPD mineralogical analyses (Fig. 5b).

SEM also provides petrographic evidence of non-clay constituents. In an examined microscopic site of the BEI bentonite sample, for instance, morphologically, the SEM micrograph shows prominent evidences of silica polymorphs; hexagonal quartz crystals were observed (Fig. 5c). However, it is likely that amorphous silica fills the space between the clay aggregates, which in turn is distinguished on the EDS spectrum by the Si and O representing silica with a background of less intense Al, Mg, and K corresponding to the clay minerals. Ca likely corresponds to the morphologically deformed micron-sized fossil fragments (Fig. 5d).

3.2.4. Specific surface area and (SSA) cation exchange capacity (CEC) analyses

Based on the MB spot test, the SSA and CEC values of the BEI whole sample are 330.3(m^2 g^{-1}) and 42.2 (meq/ 100 g), respectively. The SSA value is in the range of other bentonite samples from the eastern Iran bentonite producing zones (Modabberi et al., 2015).

With regard to the data reported for the adapted reference clays, the CEC of the BEI sample is roughly in the range of the Milos bentonite MB spot test-based measurement of CEC. The CEC value of the Wyoming bentonite (i.e. Mx-80) is much higher and is in the range of 0.7- 0.79 (meq/100 g) (Kiviranta et al., 2018). The most important factor causing relatively lower CEC in the BEI sample despite dominance of Na-montmorillonite, which typically shows higher CEC values, is the relatively lower abundances of montmorillonite and higher amounts of non-clay minerals in this sample. Furthermore, minor variations of preparation methods may cause notable difference in the measured CEC value with those of the reference bentonites. For instance, the crushing of the raw bentonite and sieving through the 2 mm pore size sieve could possibly lead to finer and more homogeneous material with higher smectite content and MB halo derived CEC (Kiviranta et al., 2018).

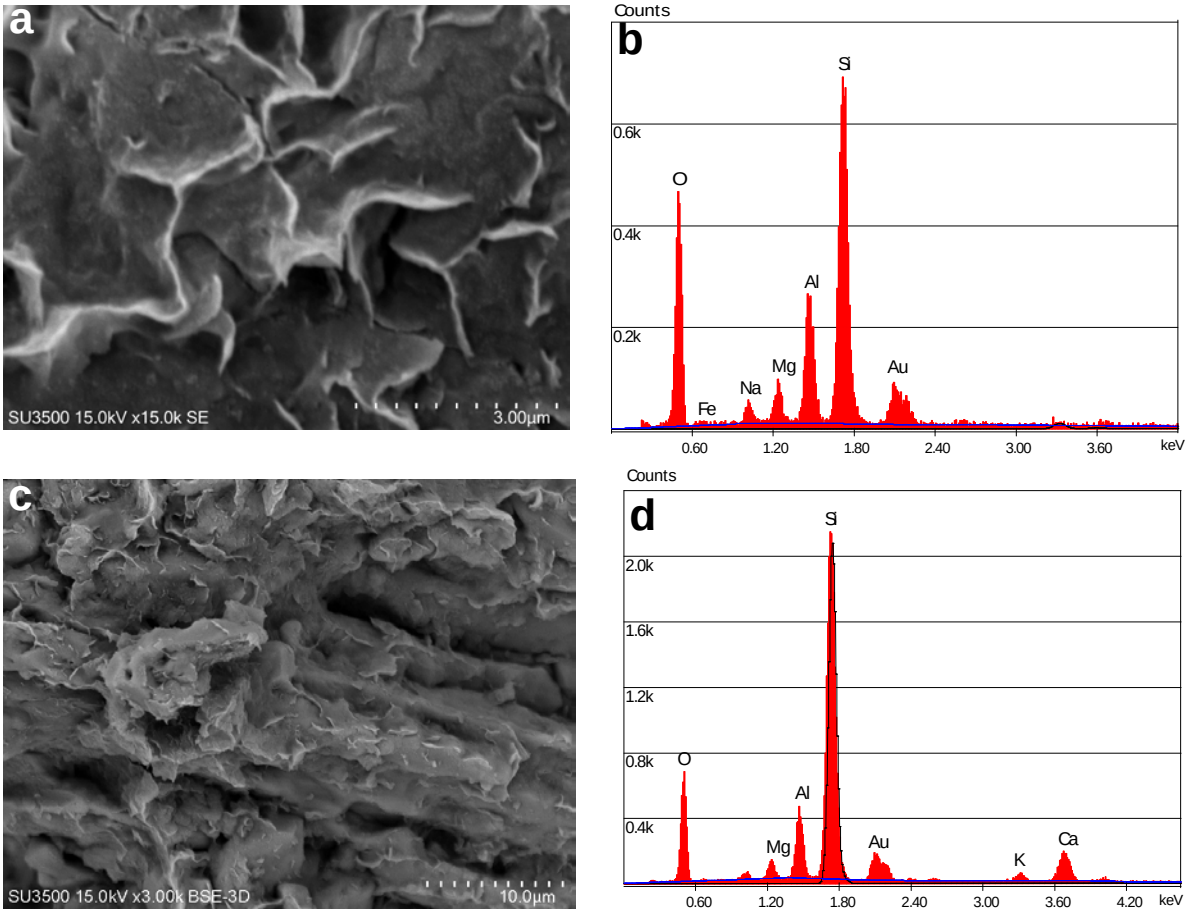

Figure 5. SEM images coupled with EDS spectra of the gold-coated BEI bentonite. The SEM is in accordance with mineralogical composition as interpreted from XRPD and FTIR spectrometry. Notable Au peaks are due to gold coating.

4. CONCLUSIONS

In this study, a bentonite from the eastern Iran, labeled as BEI, was tested for the grain size distribution, mineralogical composition, and SSA and CEC values in comparison with Wyoming and Millos bentonites as representatives for Na- and Ca-bentonites respectively. According to the results and comparisons, following conclusions can be made:

The BEI white colored bentonite comprises a very large amount of fine fraction in the whole sample and very fine fraction in the bulk sample (excluding the fraction >1 mm) is indicative of a high quality with regard to textural properties and promises wide range of applications.

XRPD, FTIR, and SEM analyses are in a good agreement with regard to identification and relative quantification of the rock forming minerals; with smectites and expandable I-S (R_0)-major minerals and calcite, silica polymorphs and zeolites as the main accessory minerals.

SSA and CEC of the whole BEI bentonite in order of the Milos bentonite, despite dominance of the Na-montmorillonite in the BEI bentonite. This is in agreement with relative abundance of non-clay minerals compared to both reference bentonites. It can be argued that, minor variations caused by partly different preparation methods may impose notable difference of the measured CEC with those of reference bentonites. For instance, the crushing of bentonite and sieving it through the 2 mm pore size sieve could cause higher CEC values in the case of the reference bentonites.

Overall, results suggest that the BEI is favorable for the energy industry applications, in particular in preparation of drilling muds and environmental maintenance related to the petroleum production and transportation. The preliminary results also promise further application of the BEI bentonite in the industries, which require more strictly controlled characteristics, such as pharmaceuticals. Nevertheless, the latter, requires further testing with regard to rheological and mechanical properties.

Acknowledgements

The authors acknowledge Dr. Friedrich Menges for providing a free academic access to the SpectraGryph

optical spectroscopy software for FTIR analyses. The authors are grateful to Dr. Oladapo Akinlotan of the University of Sussex (UK) for improvement of English of the original manuscript. H. Khadivi is acknowledged for providing the raw bentonite sample. The authors thank S. Javadi Anaghizi of Shahid Behshti University, and E. Bazyar and N.F. Nazari of Sharif University of Technology, for technical assistance during the SEM and XRD analyses.

REFERENCES

Bishop, J. L., Pieters C. M. & Edwards J. O., 1994. *Infrared spectroscopic analyses on the nature of water in montmorillonite.* Clays and Clay Minerals 42, 702-716.

Carlson, L., 2010. *Bentonite Mineralogy.* Posiva Oy, Olkiluoto, Finland.

Cheraghian, G., 2015. *Thermal Resistance and Application of Nanoclay on Polymer Flooding in Heavy Oil Recovery.* Petroleum Science and Technology 33, 1580-1586.

Çokca, E. & Birand A. A., 1993. *Determination of cation exchange capacity of clayey soils by the methylene blue test.* Geotechnical Testing Journal (GTJODJ) 16, 518–524.

Curtis, N. J., Gascooke J. R., Johnston M. R. & Pring A., 2019. *A Review of the Classification of Opal with Reference to Recent New Localities.* Minerals 9, 299.

Elzea, J. M., Odom I. E. & Miles W. J., 1994. *Distinguishing well ordered opal-CT and opal-C from high temperature cristobalite by x-ray diffraction.* Analytica Chimica Acta 286, 107-116.

Farmer, V. C. & Russell J. D., 1964. *The infra-red spectra of layer silicates.* Spectrochimica Acta 20, 1149-1173.

Graetsch, H., Gies H. & Topalović I., 1994. *NMR, XRD and IR study on microcrystalline opals.* Physics and Chemistry of Minerals 21, 166-175.

Grim, R. E. & Güven N., 1978. *Chapter 5 Properties and Uses of Bentonite.* In: Grim RE, Güven N (eds) Developments in Sedimentology, v. 24, vol 24. Elsevier, Amsterdam, The Netherlands, pp 217-248.

Heikola, T., Kumpulainen S., Vuorinen U., Kiviranta L. & Korkeakoski P., 2013. *Influence of alkaline (pH 8.3–12.0) and saline solutions on chemical, mineralogical and physical properties of two different bentonites.* Clay Minerals 48, 309-329.

Hejazi, M. & Ghorbani M., 1994. *Bentonites–Zeolite. Geological Survey of Iran (in Persian).* Geological Survey of Iran, Tehran, Iran, 128 pp.

Kandhal, P. S. & Parker F., 1998. *Aggregate tests related to asphalt concrete performance in pavements.* Transportation Research Board, Washington D.C., USA, 109 pp.

Kiviranta, L. & Kumpulainen S., 2011. *Quality control and characterization of bentonite materials.* Posiva Oy.

Kiviranta, L., Kumpulainen S., Pintado X., Karttunen P. & Schatz T., 2018. *Characterization of bentonite and clay materials 2012-2015.* vol 5. Posiva Oy, Olkiluoto, Finland.

Kumpulainen, S. & Kiviranta L., 2010. *Mineralogical and chemical characterization of various bentonite and smectite-rich clay materials.* Posiva Oy, Olkiluoto, Finland.

Kumpulainen, S. & Kiviranta L., 2011. *Mineralogical, chemical and physical study of potential buffer and backfill materials from ABM-Test Package 1.* Posiva Oy, Olkiluoto, Finland.

Madejová, J., 2003. *FTIR techniques in clay mineral studies.* Vibrational Spectroscopy 31, 1-10.

Madejová, J., Janek M., Komadel P., Herbert H. J. & Moog H. C., 2002. *'FTIR analyses of water in MX-80 bentonite compacted from high salinary salt solution systems.* Applied Clay Science 20, 255-271.

Madejová, J. & Komadel P., 2001. *Baseline studies of the clay minerals society source clays: Infrared methods.* Clays and Clay Minerals 49, 410-432.

Modabberi, S., Namayandeh A., López-Galindo A., Viseras C., Setti M. & Ranjbaran M., 2015. *Characterization of Iranian bentonites to be used as pharmaceutical materials.* Applied Clay Science 116-117, 193-201.

Moore, D. M. & Reynolds R. C., 1997. *X-ray diffraction and the identification and analysis of clay minerals.* (2nd ed). Oxford University Press, New York, USA, 376 pp.

Murray, H. H., 2006. *Applied clay mineralogy: occurrences, processing and applications of kaolins, bentonites, palygorskitesepiolite, and common clays.* (1st ed). Elsevier, Amsterdam, Netherlands, 188 pp.

Namayandeh, A., Modabberi S. & Ranjbaran M., 2015. *Mineralogical and geochemical studies to determine genesis of Khalkuh bentonite mine, Ferdows, Southern Khorasan (in Persian with an abstract in English).* Petrology 21, 19-34.

Odom, I., 1984. *Smectite clay minerals: properties and uses.* Philosophical Transactions of the Royal Society of London Series A, Mathematical and Physical Sciences 311, 391-409.

Peltonen, C., Marcussen Ø., Bjørlykke K. & Jahren J., 2008. *Mineralogical control on mudstone compaction: a study of Late Cretaceous to Early Tertiary mudstones of the Vøring and Møre basins, Norwegian Sea.* Petroleum Geoscience 14, 127-138.

Poppe, L., Paskevich V., Hathaway J. & Blackwood D., 2001. *A laboratory manual for X-ray powder diffraction: Open-File Report 2001-41.* US Geological Survey, Woods Hole, MA, 88 pp.

Ross, C. S. & Shannon E. V., 1926. *The minerals of bentonite and related clays and their physical properties.* Journal of the American Ceramic Society 9, 77-96.

Russell, J. D. & Fraser A. R., 1994. *Infrared methods.* In:

Wilson MJ (ed) Clay Mineralogy: Spectroscopic and Chemical Determinative Methods. Springer Netherlands, Dordrecht, pp 11-67.

Santamarina, J. C., Klein K. A., Wang Y. H. & Prencke E., 2002. *Specific surface: determination and relevance.* Canadian Geotechnical Journal 39, 233-241.

Yukselen, Y. & Kaya A., 2008. *Suitability of the methylene blue test for surface area, cation exchange capacity and swell potential determination of clayey soils.* Engineering Geology 102, 38-45.

Received at: 19. 01. 2021
Revised at: 09. 02. 2021
Accepted for publication at: 10. 02. 2021
Published online at: 12. 02. 2021